19th Australasian Tunnelling Conference – Acosta-Martínez, Stewart and Hudson-Smith (Eds.)

Temporary slender pillar design in low strength sandstone: A theoretical study on enhancing stability of temporary deep caverns

S. Salari, H. De Silva, M. Narayana, C. Xu
WSP, Australia

ABSTRACT: This paper presents the design and analysis of a yielding slender temporary pillar in massive sandstone at a depth of 100 metres, forming part of a temporary cavern at the base of a shaft footprint. Traditional empirical methods often result in conservative pillar designs that are unsuitable in rockmasses such as sub-horizontal bedded sandstone. To address this, the study explores the use of rock bolt reinforcement to delay brittle failure, improve energy dissipation, and change the mode of failure. Two slender temporary pillars supporting a large-span cavern were assessed using a combination of empirical design and numerical modelling. The design utilised reinforcement as a means to enhance temporary pillar confinement. This integrated design approach offers a practical alternative to conventional methods, enabling safe and efficient slender pillar construction in sub-horizontal bedded sandstone formations. The findings have implications for optimising temporary pillar dimensions and improving constructability in confined underground projects.

1 INTRODUCTION

The stability of temporary caverns in underground excavations is a critical concern for civil engineering and mining projects. This study focuses on designing ground support systems for a temporary cavern excavation, located at a depth of 100 m in sub-horizontal bedded sandstone formation. The theorised cavern, measuring 22.7 m in length, 13.6 m in width, and 7.5 m in height, is intended for spoil removal from upper levels and will be operational for 2 to 3 years before transitioning to a permanent shaft structure. Traditional empirical pillar designs, developed for mining in fractured rockmasses, often result in oversized pillars that are impractical for massive, sub-horizontal bedded sandstone formations, leading to inefficiencies in space utilization and increased construction costs.

This paper adapts the yielding pillar concept, which allows pillars to undergo controlled plastic deformation, redistributing stresses and preventing sudden inclined shear failure. The ground support system incorporates rock bolts in a pattern arrangement without shotcrete, aimed at enhancing temporary pillar confinement, yielding capacity and optimizing constructability in tight underground spaces, while also allowing the pillar to be observed. The design methodology integrates geotechnical characterization, numerical modeling using 2D finite element (RS2) and 3D finite difference (FLAC3D) methods. The study evaluates the impact of rock bolting on the temporary pillar stability through energy dissipation, delay in brittle failure post-yield, and improvement in progressive failure mode by providing a structured framework for designing temporary slender pillars in space-constrained environments. The remaining parts of this paper are as follows, literature review (section 2), Design methodology (section 3), discussion on temporary pillar stability analysis including empirical approaches and numerical assessment in 2D and 3D (sections 4 and 5), and conclusion on main findings of the current study (section 6).

2 LITERATURE REVIEW: SLENDER PILLARS IN TUNNELLING

The yielding pillar concept, pioneered in room and pillar mining, allows pillars to undergo controlled plastic deformation, absorbing energy and maintaining residual strength to prevent catastrophic failure (Salamon, 1970). This approach enables stress redistribution from the pillar core to surrounding rock, creating a destressed zone that enhances overall excavation stability (Yavuz, 2001). Yielding pillars have been extensively studied in coal and soft rock mining, where they accommodate large deformations without sudden collapse (Esterhuizen et al., 2011) as shown in

Figure 1, unlike the sudden brittle failure shown in Figure 2 (Renani & Martin, 2018). Esterhuizen et al. demonstrated that yielding pillars in coal measures can reduce roof-to-floor convergence by allowing controlled yielding, which is particularly effective in weak rockmasses.

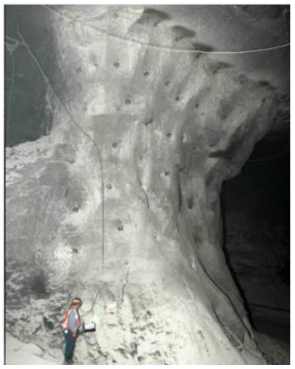

Figure 1: Pillar covered by wiremesh and bolts to prevent sudden brittle failure (Esterhuizen et al., 2011)

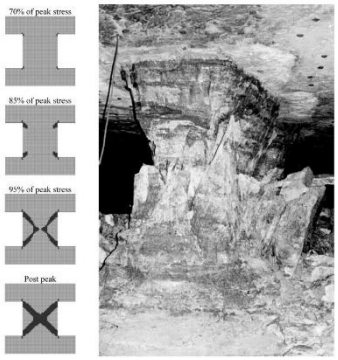

Figure 2: Progressive failure of hard rock pillars (Renani & Martin, 2018)

Martin & Maybee (2000) provided empirical formulas for pillar strength reduction and stability assessment in hard rock mines, which have been widely used in the industry. Their work highlighted the importance of considering the width-to-height ratio and rockmass quality in pillar design. Empirical pillar design methods, such as those by Lunder & Pakalnis (1997), rely on case histories from fractured rockmasses and are often conservative, leading to overdesigned pillars (Martin & Maybee, 2000). These methods underestimate the strength of massive rockmasses, resulting in oversized pillars that reduce usable space and increase construction costs. The application of yielding pillars in civil tunnelling, particularly in massive sandstone, have been recently studied (Thirukumaran & Oliveira, 2023). Employing 3D analysis, slender rock pillars formed in large span road tunnels and cavern Y-junctions in Hawkesbury Sandstone have been studied, combining numerical modeling with empirical methods to ensure pillar stability under high stress conditions. This highlighted the effectiveness of slender pillars in space-constrained environments, supported by rock bolting to enhance ductility. Dressel & Diederichs (2022) investigated the influence of rockmass parameters and yield criterion on pillar design. Their work suggested that 3D numerical modelling can capture the complex interactions between rockmass properties and pillar stability. Hamediazad & Bahrani (2024) evaluated the rock mass strength for hard rock pillar design using bonded block models. Sinha & Walton (2019) conducted numerical analyses of pillar behaviour, varying yield criteria, dilatancy, rock heterogeneity, and length-to-width ratios, to understand the complex interactions that influence pillar stability.

This paper builds upon the yielding pillar framework and adapts it for use in civil tunnelling through massive sandstone. A hybrid design methodology is presented, integrating empirical classification, numerical stress modelling, and practical reinforcement strategies, such as GRP bolts and pattern bolting, to achieve controlled yielding and maintain temporary pillar stability throughout the excavation's operational phase.

3 DESIGN METHODOLOGY

The design methodology adopted in this study integrates empirical and numerical approaches to assess the stability and performance of slender temporary pillars. Furthermore, a numerical pillar compression test was carried out for temporary pillar assessment. Temporary pillar stability in the design of the shaft cavern (a temporary cavern formed at the base of a shaft footprint) has been assessed using the following four methods:

- Pillar strength factor obtained from 2D assessment (RS2)
- Pillar stress assessment in 3D (FLAC 3D)
- Examining of pillar through an empirical approach
- Use of GRP rockbolts to improve failure mode and energy dissipation

3.1 *Ground conditions*

Design parameters for the low strength sandstone rock mass class are listed in Table 1. The groundwater table is significantly below the cavern, eliminating hydrostatic pressure considerations. Bedding and joint set with dip / dip direction of 5°/340° and 85°/220°, respectively was considered.

Table 1: Material properties

Parameter		Value
UCS		12 MPa
Intact Rock Modulus (Ei)		3500 MPa
Unit Weight		23 kN/m^3
Mass Rock Modulus (Em)		3100 MPa
K_0		0.5
Generalised Hoek Brown	mb	8.322
	s	0.108
	a	0.501
Equivalent Mohr Coulomb	ϕ	50°
	C	619 kPa

3.2 *Temporary Cavern and pillar geometry*

The temporary cavern measures 22.7 m in length, 13.6 m in width, and 7.5 m in height, as depicted in Figure 3, with temporary pillar 1 and pillar 2 dimensions as shown in Table 2.

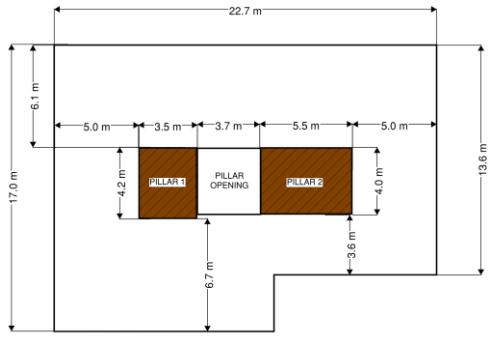

Figure 3: Plan view of Shaft Cavern (Dimensions are in m)

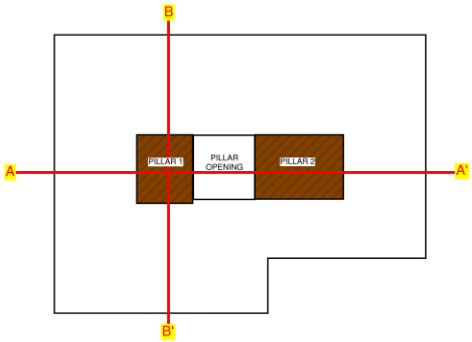

Figure 4 : 2D design analysis sections

Table 2: Temporary pillar dimensions

Pillar No	Pillar Width, W(m)	Pillar Length, L(m)	Pillar Height, H(m)	W/H
1	3.5	4.25	7.5	0.47
2	4.0	5.5	7.5	0.53

3.3 *Modelling approach*

A comprehensive approach was adopted to evaluate the stability of the slender temporary pillars under high-stress conditions. Initially, a two-dimensional finite element analysis was carried out using RS2 software (Rocscience) to further assess the stability of key excavation sections and the effectiveness of proposed support systems. Two critical cross-sections (AA' and BB'), as shown in Figure 4, were selected to analyse the two slender temporary pillars, incorporating staged excavation sequences and rock bolt interaction to accurately reflect construction conditions.

Following the stress analysis from RS2, a three-dimensional numerical model was developed using FLAC3D, which is a finite difference program by Itasca, to simulate temporary pillar stress distribution and identify zones of elevated stress concentrations. Empirical methods based on the work of Martin and Maybee (2000) and Esterhuizen et al. (2011) were then applied to assess the pillar strength, with results indicating a factor of safety slightly below one. Field measurements

of mine pillars have demonstrated that yielding within specific width ranges can potentially enhance pillar strength (Yavuz, 2001), an aspect not considered in the current design where the rock material is limited to elastic behaviour. While yielding may, in certain cases, contribute to the overall strength of the system, this section focuses specifically on the application of pattern bolts to improve the temporary pillar's confinement and post-yield capacity. Further 3D modelling of the pillar in a compression test was undertaken to assess the pillar response to understand the behaviuor of the temporary pillar under the high stress loading conditions.

The geometry and mesh generation of the critical pillar in FLAC3D with the dimension of 4.25 m in length, 3.5 m in width, and 7.5 m in height is described in Figure 5. Furthermore, an elastic-plastic Strain softening Mohr-Coulomb model is introduced employing equivalent Mohr-Coulomb parameters shown in Table 1 with a residual friction angle, $\phi_R = 35^{\circ}$, residual cohesion, $C = 0.0619$ (MPa), and tensile cut-off as $T = 100$ (kPa). The strain softening behaviour is controlled by adopting the parameters provided in Table 3.

Table 3: Mohr-Coulomb Parameters for Strain Softening Model

Strain	0	0.005	0.0051	1
Cohesion (kPa)	619	619	61	61
Friction angle (°)	50	50	35	35
Tensile strength (kPa)	100	100	10	10

For support cases, GRP pattern bolts are installed at the pillar. To capture the post-yield behaviour of the temporary pillar, a displacement-controlled test is conducted using FLAC3D. In this analysis, a total displacement of 35 mm is applied, with increment size of 0.001 mm per step.

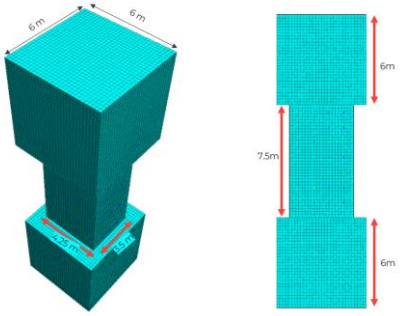

Figure 5: Geometry and Mesh of the Critical Temporary Pillar (Pillar 1)

4 TEMPORARY PILLAR STABILITY ANALYSIS RESULTS

4.1 *Pillar Stress Assessment (FLAC3D)*

The temporary pillar stress distribution in 3D due to high stress loading condition is illustrated in Figure 6. The stress distribution results are analysed across five distinct sections, as defined by the plan illustrated in Figure 7.

Based on the evaluation of stress results in the pillar zone across different sections, it is estimated that high-stress conditions will exist in all sections of the pillar. As shown in Figure 8 and Figure 9, consistently high average stress levels are seen across the entire temporary pillar zone (more than 4 MPa), potentially leading to localized yielding. To address this issue, the initial solution involves the use of pattern bolting to enhance confinement and control brittle deformation, so that yielding of the temporary pillar is controlled. The effectiveness of this approach in enhancing pillar performance is discussed in detail in Section 4.4. For additional safety, impact barriers and a wire mesh around the pillars will be installed. Given the high-stress levels identified in the temporary pillar zones of both Pillar 1 and Pillar 2, the installation of 6-metre-long crown bolts are used to stabilize the cavern under a yielding pillar condition. These bolts are designed to enhance crown stability during temporary pillar yielding by redistributing stresses from the pillar zone to the abutments through the arching action of the compression beam above the crown.

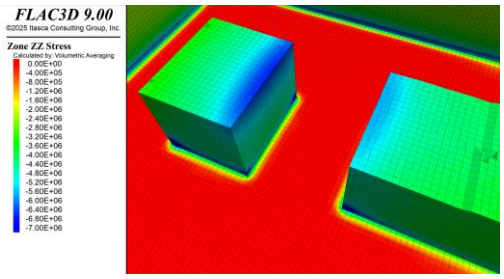

Figure 6: Temporary pillar assessment under stress σ_{zz} (Pa), loading condition in FLAC3D

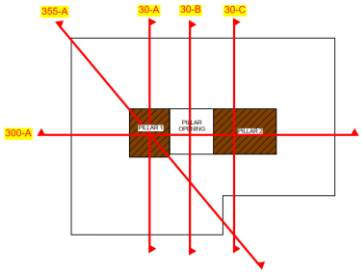

Figure 7: Critical cross sections in FLAC3D model

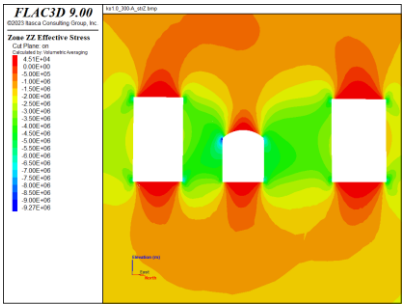

Figure 8: Vertical Stress distribution contour, σ_{zz} (Pa), at pillar zone Section 300-A

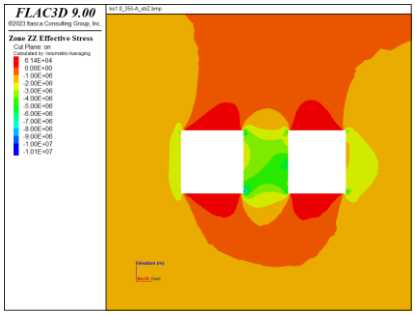

Figure 9: Vertical Stress distribution contour, σ_{zz} (Pa), at pillar zone Section 355-A

4.2 *Temporary Pillar stability – Empirical approach*

Empirical formulas from Martin and Maybee (2000) and Esterhuizen et al. (2011) were used to estimate pillar strength and Factor of Safety (FOS). Pillar stability assessment is typically carried out by estimating the pillar strength and stress and then estimating the margin that exists between the expected pillar strength and stress. The FOS relates the average pillar strength (S) to the average pillar stress (σ_p) as follows,

$$FOS = \frac{S}{\sigma_p} \tag{1}$$

Figure 10 shows a comparison of different empirical formulas used for pillar strength.

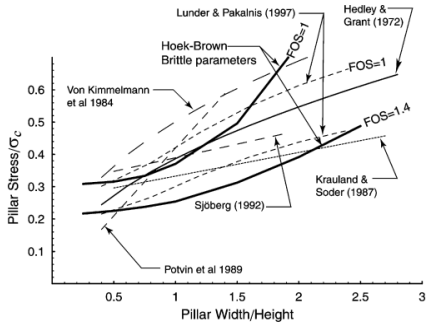

Figure 10: Hard-rock pillar stability and elastic 2D models using Hoek-Brown brittle parameters (Martin & Maybee, 2000).

The average temporary pillar stress (σ_p) is estimated through numerical modelling varies from 4.0 MPa to 4.3 MPa. Table 4 shows the FOS of Pillar 1 and 2 based on the numerical analysis detailed in the FLAC3D elastic model. To verify the outcomes of the pillar strength estimated from the numerical analyses, the relationship developed by Martin and Maybee is also used to estimate the pillar strength (Martin & Maybee, 2000). As can be seen from Table 4 below, the Factor of Safety is less than 1 for the applied stress condition using empirical charts. This indicates the need to increase pillar width.

Table 4:Results of temporary pillar stability assessment

Pillar No	W (m)	H (m)	UCS (MPa)	Average Pillar Stress (MPa) FLAC3D elastic	Martin and Maybee (2000)			Esterhuizen et al. (2011)	
					Reduction factor	Pillar strength, *S* (MPa)	FOS	Pillar strength, *S* (MPa)	FOS
1	3.5	7.5	12	4.3	0.32	3.8	0.90	3.5	0.80
2	4.0	7.5	12	4.0	0.32	3.8	0.95	3.6	0.90

4.3 *RS2 Modelling of Temporary pillar*

A temporary pillar assessment has been undertaken using the design sections shown in Figure 4. The pillar stresses are extracted from the RS2 finite element model (FEM), as shown in Figure 11 and Figure 12. Both temporary pillars, particularly in their lower half, exhibit yielding, requiring: 1- pattern bolting on pillars; 2- longer bolts at the crown; and 3- reinforcement mesh to the bottom section of the pillar sidewalls. As discussed previously, these measures are critical to ensuring stability and mitigating the effects of localized yielding in the pillar zones.

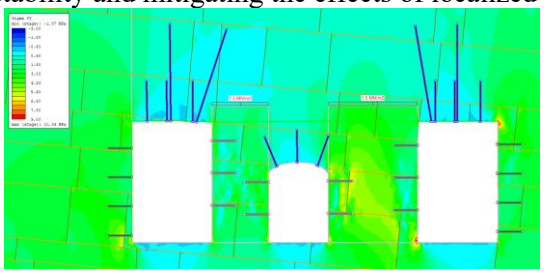

Figure 11: Vertical stress distribution (MPa) in RS2 for section AA': Pillar 1, 2, and opening

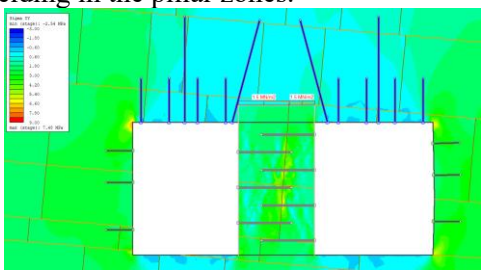

Figure 12: Vertical stress distribution (MPa) in RS2 for section BB': Pillar 1

4.4 *Temporary Pillar bolting- FLAC3D Assessment*

To further understand temporary pillar yielding behavior, a stress-displacement curve has been plotted in Figure 13 to compare the post-yield response and the nature of failure when using GRP bolts. The analysis suggests that the introduction of GRP bolts has improved the failure mode of the temporary pillar, enabling slightly more deformation post yield. It highlights that the temporary pillar with GRP bolt support is provided the benefit of additional displacement before reaching failure. The GRP-reinforced pillar shows a delay in the onset of brittle failure by approximately 3 mm (when comparing plastic portion - refer to Figure 13: (1) Without GRP: 2.5 mm; (2) with GRP: 5.5 mm, which, although small, resulted in measurable energy dissipation.

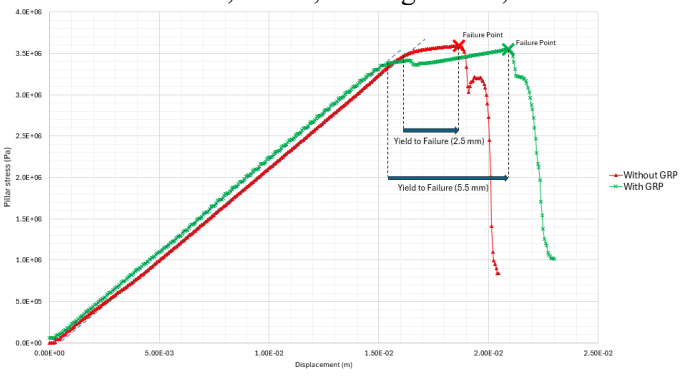

Figure 13: Pillar Strength (Pa) vs Applied Displacement (m), Impact of GRPs on delaying failure

Additionally, relative energy dissipation capacity is increased by approximately 22% before failure due to the inclusion of GRP, referring to the following energy graph in Figure 14.

$$\delta_E = \frac{E_{with\ GRP} - E_{without\ GRP}}{E_{without\ GRP}} \cong 22\% \quad (2)$$

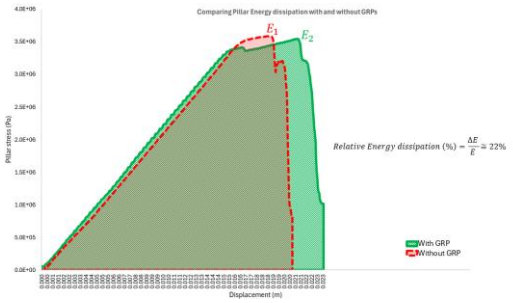

Figure 14: Energy dissipation comparison of the temporary pillar with and without GRPs

Deformation and failure mechanisms of temporary pillar cases, with and without GRP bolts are illustrated in Figure 15 and Figure 16 which shows improvement in post yielding deformation of the temporary pillar while using GRP bolts. The mode of failure using GRP bolts has changed from inclined shear failure to progressive crushing failure, which provides additional time for assessing and monitoring temporary pillar condition at critical stages of excavation.

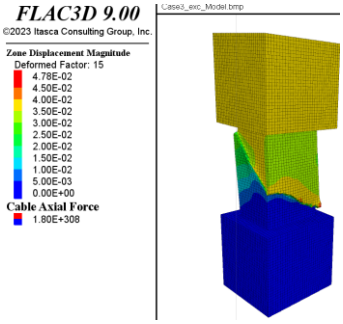

Figure 15: Deformation (m) and Failure Mechanism in Pillar; Case 1- without Support leading to inclined shear failure mode

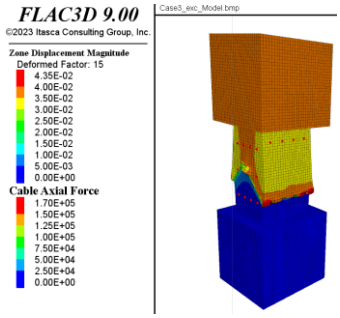

Figure 16: Bolt axial force (N), deformation (m) and Failure Mechanism in Pillar; Case 2- using GRPs leading to progressive crushing failure mode

To examine bolts capacity, the axial force in the GRP bolt pattern is described in Figure 17 and Figure 18 with a maximum value of 170 kN. Maximum principal strain and deformation contours are shown in Figure 17 and Figure 18 respectively. In the current pillar test, the temporary pillar does not exhibit a significant strength gain. However, this limitation is primarily due to the adopted rock mass parameters and adopted strain-softening material model in this experiment, which is more focused on understanding the impact of GRP bolts post-yield behavior. More advanced strain-softening constitutive models can be adopted to better capture the post-peak performance of temporary pillars, as demonstrated in previous studies (e.g., Cammarata et al., 2023; Thirukumaran & Oliveira, 2023). Further assessment, incorporating field mapping, monitoring data and the observed rock mass conditions in massive sandstone, can improve capacity expectations of temporary pillars and forms part of the observational approach in the current design.

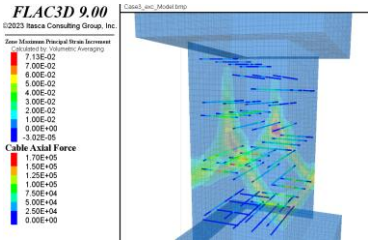

Figure 17: Maximum principal strain and GRP bolt axial force contours (N)

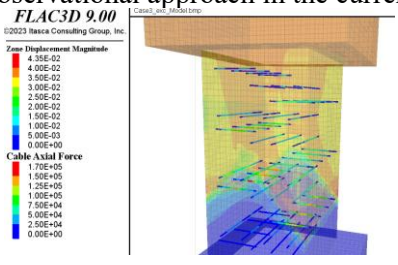

Figure 18: Displacement magnitude (m) and GRP bolt axial force contours (N)

5 SUPPORT STRATEGIES FOR SLENDER TEMPORARY PILLARS

To address the identified yielding and potential instability of slender temporary pillars, a targeted support strategy was implemented. This included GRP bolts, and pattern bolting configured to improve the post yield response and control the mode of failure by adding confinement. The

change from an inclined shear failure to progressive crushing failure provides an additional level of safety by providing the opportunity to observe the effects of overstress and implement mitigation actions. A displacement-controlled FLAC3D analysis demonstrated that GRP bolts delay the onset of failure and enable increased energy dissipation. To account for the risk of brittle failure, 6 m bolts can be proposed at the crown, as a precaution. This allowed the crown to function as a compression arch, redistributing stresses and enhancing global cavern stability in case of yielding. Wire mesh reinforcement could be recommended particularly near the base of the temporary pillars to control rock fall hazards. This provided surface confinement and support against rock spalling.

6 CONCLUSION

This approach developed a structured framework for designing and assessing slender temporary pillars with bolting, aiming to provide more optimised pillar sizes and move away from purely empirical performance-based design. Traditional empirical methods have been developed based on mining in fractured rockmasses and the data is from case histories in the mining industry, leading to large pillars in rockmasses where the methods may yield conservative pillar sizes. The design method adopted in this paper can be employed to optimize temporary pillar dimensions in tight underground areas, where optimal space proofing is crucial for constructability reasons, and risks associated with pillar yielding can be foreseen via the use of numerical modelling tools, and a good understanding of rockmasses where defects are minimal. The use of GRP pattern bolts and mesh wrapping provided essential confinement and energy dissipation, effectively managing the mode of failure transitions from an inclined shear failure to progressive crushing failure in the temporary pillar response. Additionally, the incorporation of longer bolts in the crown facilitated the redistribution of stress away from the pillars, further enhancing cavern stability even in case temporary pillar yields. Progressive failure mode provides additional time to monitor temporary pillar conditions during critical stages of excavation, highlighting the importance of incorporating an instrumentation and monitoring plan into the design phase. For future studies, it is recommended that more advanced constitutive models (e.g., advanced strain-softening or damage-plasticity models) be developed to better capture fracture mechanics, post peak response, and load transfer mechanisms between the rock mass and reinforcement.

7 REFERENCES

Dressel, E.J. and Diederichs, M.S., 2022. A numerical investigation on the influence of rockmass parameters and yield mechanics in pillar design. *The Evolution of Geotech*, p.492. doi:10.1201/9781003188339-62.

Cammarata, G., Elmo, D. and Brasile, S., 2023. Modelling of progressive failure mechanism of mine pillars. *In IOP Conference Series: Earth and Environmental Science* (Vol. 1124, No. 1, p. 012099). IOP Publishing.

Esterhuizen, G.S., Dolinar, D.R. and Ellenberger, J.L., 2011. Pillar strength in underground stone mines in the United States. *International Journal of Rock Mechanics and Mining Sciences*, *48*(1), pp.42-50. https://doi.org/10.1016/j.ijrmms.2010.06.003

Hamediazad, F. and Bahrani, N., 2024. Evaluation of the rock mass strength for hard rock pillar design using bonded block models. *Rock Mechanics and Rock Engineering*, *57*(5), pp.3659-3680.

Martin, C.D. and Maybee, W.G., 2000. The strength of hard-rock pillars. *International Journal of Rock Mechanics and Mining Sciences*, *37*(8), pp.1239-1246. https://doi.org/10.1016/S1365-1609(00)00032-0

Renani, H.R. and Martin, C.D., 2018. Modeling the progressive failure of hard rock pillars. *Tunnelling and Underground Space Technology*, *74*, pp.71-81. https://doi.org/10.1016/j.tust.2018.01.006

Salamon, M.D.G., 1970, November. Stability, instability and design of pillar workings. In *International journal of rock mechanics and mining sciences & geomechanics abstracts* (Vol. 7, No. 6, pp. 613-631). Pergamon. https://doi.org/10.1016/0148-9062(70)90022-7

Sinha, S. and Walton, G., 2019. Numerical analyses of pillar behavior with variation in yield criterion, dilatancy, rock heterogeneity and length to width ratio. *Journal of Rock Mechanics and Geotechnical Engineering*, *11*(1), pp.46-60. https://doi.org/10.1016/j.jrmge.2018.07.003

Thirukumaran, S. and Oliveira, D., 2023. Innovative design of slender rock pillar formed within large span road tunnels and cavern Y-junction in Hawkesbury Sandstone. *Tunnelling and Underground Space Technology*, *141*, p.105376. https://doi.org/10.1016/j.tust.2023.105376

Yavuz, H., 2001, June. Yielding pillar concept and its design. In *17th International mining congress and exhibition of Turkey-MCET* (pp. 397-404).